Variability and Order in Cytoskeletal Dynamics of Motile Amoeboid Cells

Hsin-Fang Hsu,[1] Eberhard Bodenschatz,[1,2,3,*] Christian Westendorf,[1] Azam Gholami,[1] Alain Pumir,[1,4] Marco Tarantola,[1] and Carsten Beta[1,5,†]

[1]*Max Planck Institute for Dynamics and Self-Organization (MPIDS), D-37077 Göttingen, Germany*
[2]*Institute for Nonlinear Dynamics, University of Göttingen, D-37073 Göttingen, Germany*
[3]*Laboratory of Atomic and Solid-State Physics and Sibley School of Mechanical and Aerospace Engineering, Cornell University, Ithaca, New York 14853, USA*
[4]*Université Lyon, ENS de Lyon, Université Claude Bernard, CNRS, Laboratoire de Physique, F-69342 Lyon, France*
[5]*Institute of Physics and Astronomy, University of Potsdam, D-14476 Potsdam, Germany*

(Received 2 June 2016; published 6 October 2017)

The chemotactic motion of eukaryotic cells such as leukocytes or metastatic cancer cells relies on membrane protrusions driven by the polymerization and depolymerization of actin. Here we show that the response of the actin system to a receptor stimulus is subject to a threshold value that varies strongly from cell to cell. Above the threshold, we observe pronounced cell-to-cell variability in the response amplitude. The polymerization time, however, is almost constant over the entire range of response amplitudes, while the depolymerization time increases with increasing amplitude. We show that cell-to-cell variability in the response amplitude correlates with the amount of Arp2/3, a protein that enhances actin polymerization. A time-delayed feedback model for the cortical actin concentration is consistent with all our observations and confirms the role of Arp2/3 in the observed cell-to-cell variability. Taken together, our observations highlight robust regulation of the actin response that enables a reliable timing of cell movement.

DOI: 10.1103/PhysRevLett.119.148101

Cell motility is an essential biological function that drives a wide range of processes as diverse as the foraging of microorganisms, the healing of a wound, or the metastasis of cancer cells [1,2]. It relies on coordinated sequences of membrane protrusion, adhesion, and retraction that are tightly orchestrated by the dynamics of the actomyosin cytoskeleton. The latter shows remarkable signs of self-organization, such as autonomous oscillations, coherent wave patterns, and the emergence of characteristic length and time scales of membrane protrusions [3–5]. Self-organization in the actomyosin cytoskeleton was studied in different eukaryotic systems. Among them, the social amoeba *Dictyostelium discoideum* became a widely used model, due to its many homologies with motile mammalian cells [6].

In many cases, actin-based locomotion of cells is directionally biased by chemotactic cues [7–10]. They are typically transmitted via transmembrane receptors and associated signaling pathways to the actomyosin cytoskeleton to guide motility toward specific target sites such as the movement of leukocytes to places of injury [11]. Gradient responses of amoeboid cells are highly robust over several orders of magnitude in gradient steepness and background concentration [12]. How are these remarkable properties controlled at the cytoskeletal level of individual cells?

In recent years, it became increasingly clear that substantial cell-to-cell variability may occur even within a population of genetically identical cells [13–15]. In this work, we focus on cell-to-cell variability in the actin response to extracellular chemoattractant stimuli, by systematically varying the concentration of external cAMP applied to chemotactic *Dictyostelium* cells. We elucidate how robust features emerge from the large spread of single-cell responses. Finally, we propose an underlying mechanism and capture our observations with a simple mathematical model.

Experimental procedures.—We combined microfluidic flow photolysis with multicolor confocal microscopy to record cytoskeletal dynamics in single *Dictyostelium* cells in the presence of well-controlled chemical stimuli. We visualized actin dynamics by expressing fluorescently tagged DdLimEΔcoil (LimE-GFP), which is known to colocalize with freshly polymerized actin filaments [16,17]. Stimuli with the chemoattractant cAMP were generated by laser-induced release from a caged precursor in a flow that transports cAMP to the cell of interest. This method allowed us to control the cAMP stimulus with a high spatiotemporal resolution [18–20].

Actin polymerization close to the cell membrane, denoted as the cortex, results in pseudopods driving cell motion. This induces strong spatial heterogeneities in actin polymerization. On the contrary, in the interior (i.e., in the cytosol), the fluorescence marker is well mixed. Therefore, in this study the fluorescence intensity of LimE-GFP in the cytosolic region is considered as the response signal, as it reflects the global dynamics in the cell: Enhanced polymerization in the cortex leads to a weaker LimE-GFP fluorescence signal in the cytosol and vice versa. The total fluorescence signal in the cytosolic region is always averaged over the corresponding area. For a comparison among different cells, every response is divided by the average intensity before stimulus.

Finally, the signal is shifted such that the average intensity before stimulation is 1.

In response to a 1 s cAMP stimulation, actin polymerization is transiently enhanced in the cortex. The temporary recruitment of LimE-GFP to the cell cortex results in a decrease in the cytosolic signal [Fig. 1(a)]. The following depolymerization of the cortical actin then leads to an increase in the cytosolic signal. We quantified the cytosolic signal by three parameters: the response amplitude (A) and the response intervals dominated by polymerization (T_p) and depolymerization (T_d); see Fig. 1(a). After T_d, the reliable detection of the signal usually becomes difficult. These definitions can be extended to the responses of other markers, such as Aip1 (actin-interacting protein) or Arp2/3 (actin-related protein), where they denote the amplitude and the recruitment and dissociation times of the respective proteins to and from the cortex.

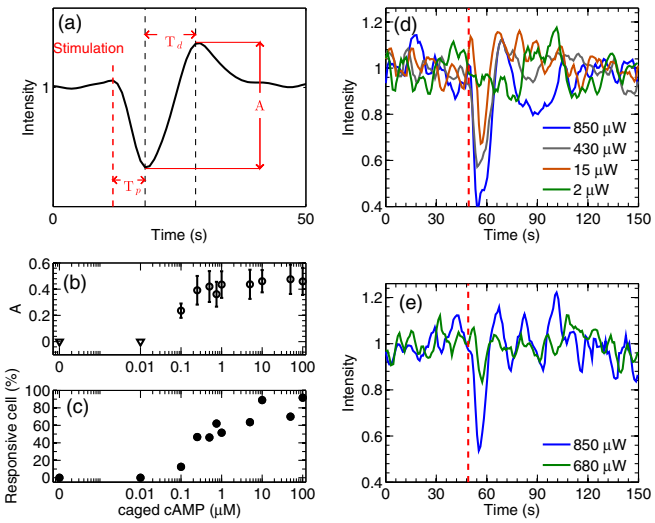

FIG. 1. Responses to a cAMP stimulation. The signal, normalized as explained in the text, is defined as responsive when the difference between the intensity before cAMP stimulation and the minimum intensity after stimulation is larger than the intensity variations before stimulation (i.e., mean $-2\times$ std). (a) A schematic diagram showing parameters that characterize the actin response. The polymerization time T_p is defined as the time between the stimulus (red dashed line) and the intensity minimum. The depolymerization time T_d is defined as the time between the extrema (valley to peak) in cytosolic intensity (between gray dashed lines). The amplitude A is defined as the difference in intensity between the peak and valley. (b) Average response amplitude A, defined as in (a), at different stimulation strengths. For each concentration, experiments on more than ten cells were carried out. For caged cAMP concentrations larger than 0.1 μM, only signals from responsive cells were averaged. Error bars denote the standard deviation. A is set to zero for 0 and 0.01 μM caged cAMP as no cells responded (triangle). (c) Dependence of the percentage of responsive cells on the concentration of caged cAMP. For each concentration, experiments on more than ten cells were carried out. (d), (e) Examples of responses to different stimulation strengths in two cells. Different colors show the responses to different cAMP concentrations that were generated by releasing cAMP with different powers of the uncaging laser as indicated in the legend. The red dashed line indicates the time of stimulation.

A cell-specific threshold governs the response to external stimuli.—We first investigated how the actin response depends on the strength of the cAMP stimulus by averaging response signals from responsive cells at various stimulation strengths. Figure 1(b) shows that the averaged response amplitude displays a threshold behavior. Above the threshold, it first increases with increasing stimulation strength (10 to 250 nM) and then scatters around a plateau (250 nM to 100 μM). Moreover, the percentage of responsive cells also increases with the strength of stimulation [Fig. 1(c)], implying a cell-specific threshold value.

We next determined the response threshold of individual cells by successively adjusting the power of the uncaging laser to apply different cAMP concentrations to the same cell with a waiting time of 4 min between stimulations, which is significantly longer than the time interval of approximately 50 s necessary for the cells to fully recover [18]. The lowest stimulation strength to which a cell responded is regarded as the threshold value. We observed that the threshold can vary from cell to cell over a large range of the uncaging laser power [from 15 to 680 μW, Figs. 1(d) and 1(e)]. In our experimental setup, the level of cAMP released at a given laser power can be only indirectly inferred by a comparison with similar response curves from the literature [13]. Still, our experiments allow us to reliably explore qualitative trends that occur when the cAMP concentration is changed.

Above the threshold, response amplitudes and polymerization time scales show strong cell-to-cell variations.—To further investigate the cellular response in the plateau region [Fig. 1(b)], we quantified the individual responses of 101 cells to a strong stimulation (i.e., by exposing a 10 μM caged cAMP solution to an 850 μW laser pulse, which allows most cells to reach the plateau on the response curve). Their response amplitudes and depolymerization times vary over a wide range, while the polymerization time is closely confined to values around 6 s; see Fig. 2. This observation is in line with earlier results showing variability in the response of the upstream signaling pathway under the same strength of stimulation [14]. By repeatedly stimulating the same cell with the same cAMP concentration, we found that variations in the response amplitude may be attributed to intrinsic noise within the cells [21].

In *D. discoideum*, spontaneous oscillations in actin polymerization with a period of around 10 s have been reported [18,24–26]. Therefore, we tested whether the dynamical state of the actin system prior to the stimulus affects the response characteristics. We compared the responses of cells showing oscillations 50 s prior to cAMP stimulation with cells that did not oscillate and observed similar behavior [21]. This indicates that the

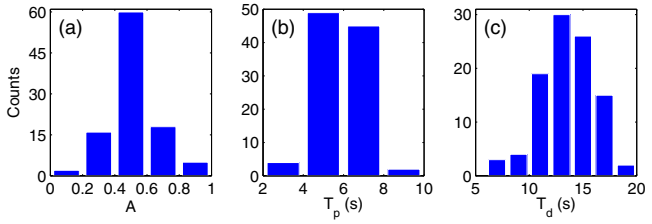

FIG. 2. Characteristics of the actin response to cAMP stimulation. $N = 101$ cells. (a) Histogram of A (mean $\pm$ std $= 0.5 \pm 0.15$). (b) Histogram of T_p (mean $\pm$ std $= 5.7 \pm 1.05$). (c) Histogram of T_d (mean $\pm$ std $= 13.4 \pm 3.25$).

presence of oscillations has no influence on the cAMP response and is not related to the cell-to-cell variability we observed. Rather, upon an external chemoattractant stimulus, spontaneous actin oscillations are immediately replaced by the response to the chemical stimulus. Overall, the existence of a threshold of excitation, and of a response which is independent of the stimulation above the threshold (up to noise effects), is consistent with the notion that the signal transduction system is excitable [24].

Response amplitude sets response frequency.—Despite pronounced cell-to-cell variability, we observed clear relations between the response amplitude and the polymerization and depolymerization times. First, the polymerization time was found to be almost independent of the amplitude A: $T_p = 6.2 \pm 1.0$ s in $N = 136$ cells; see Fig. 3(a). The depolymerization time T_d, on the other hand, increases with increasing A; see Fig. 3(b). This way, the duration of the full response is prolonged for larger values of A. This explains the previously observed discrepancy between the period of spontaneous oscillations (around 10 s) [24] and the resonance period of forced oscillations (around 20 s) [18]. The depolymerization time is longer in the case of stimulated responses, as the amplitude of stimulated responses is typically much larger than the amplitude of spontaneous oscillations. This results in prolonged response intervals and thus in a shift of the resonance peak to longer periods [18].

Relation between Arp2/3 *activation and cell-to-cell variability.*—What is the origin of cell-to-cell variability in the response amplitude, even though the polymerization time is constant in different cells? To answer this question, we studied regulators of actin polymerization and depolymerization with respect to the amount of their cortical localization. As representative examples, we have chosen the Arp2/3 complex that enhances actin polymerization by the creation of new barbed ends and Aip1 that enhances actin depolymerization [27]. We observed that the actin amplitude and thus the depolymerization time T_d are correlated with the amount of Arp2/3 in the cortex as can be seen in Figs. 3(c) and 3(d). Furthermore, the dependencies of $T_{p,\mathrm{Arp2/3}}$ and $T_{d,\mathrm{Arp2/3}}$ on $A_{\mathrm{Arp2/3}}$ [21] are qualitatively similar to those of T_p and T_d on A that characterize the actin response and are shown in Figs. 3(a) and 3(b). Taken together, these two observations point to a strong role of Arp2/3 in the observed cell-to-cell variability of the actin response in the cortex. Upon treatment with low concentrations of the Arp2/3 inhibitor CK666 (5 and 10 μM), the dependence of the actin amplitude on the amount of cortical Arp2/3 shows only moderate changes. We merely observed that an increased amount of Arp2/3 is required to achieve a given level of actin polymerization [21]. This is once again consistent with the notion that the amount of Arp2/3 determines the actin response. For a high CK666 concentration (100 μM), cytoskeletal activity is disrupted, and the majority of cells do not show any actin response when exposed to a cAMP stimulus [21].

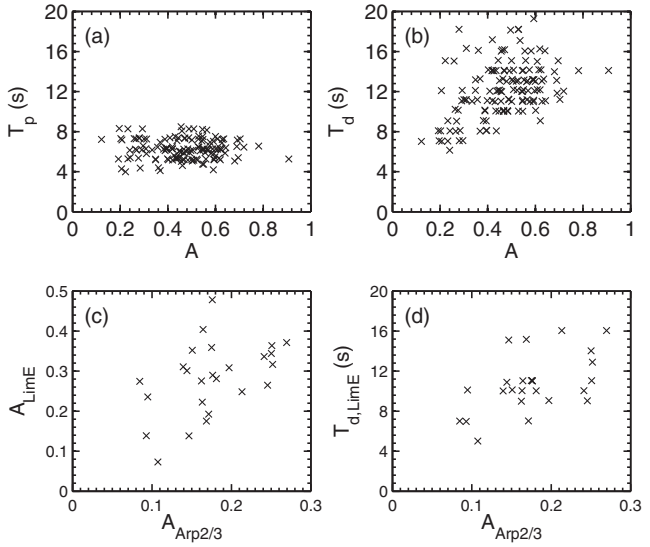

FIG. 3. Signatures of the response to cAMP stimulation. Each black cross shows the response of one cell to a single stimulus. The parameters are always defined as in Fig. 1(a). (a) Relation between the polymerization time and response amplitude ($N = 102$ cells, Pearson product-moment correlation coefficient $\rho = -0.02$). (b) Relation between the depolymerization time and response amplitude ($N = 102$ cells, $\rho = 0.42$). (c) Amplitude relation between Arp2/3 and LimE ($N = 25$ cells coexpressing Arp2/3-GFP and LimE-mRFP, $\rho = 0.46$). (d) Relation between the actin depolymerization time and the amplitude of Arp2/3 ($N = 25$ cells coexpressing Arp2/3-GFP and LimE-mRFP, $\rho = 0.51$).

Also for Aip1, similar dependencies of the recruitment and dissociation times $T_{p,\mathrm{Aip}}$ and $T_{d,\mathrm{Aip}}$ on the amplitude A_{Aip} are observed. In contrast to Arp2/3, however, the association time $T_{p,\mathrm{Aip}}$ is shifted to larger values, as is expected for a regulator of actin depolymerization [21].

What is setting the constant polymerization time? Capping protein, which is a terminator of actin polymerization, is abundantly available in *D. discoideum* [28,29]. It diffuses fast within the cell [30] and shows a high affinity to the barbed ends of actin filaments [28]. Therefore, binding to the barbed ends is expected to occur within 1 s, which is much shorter than the polymerization time we observed

(6.1 ± 1.1 s). The constant polymerization time may be rather controlled from the very beginning of the signaling cascade, as cAMP stimulation also activates G proteins with a similar time scale [31–33].

Finally, the dependence of the depolymerization time on the response amplitude reflects the fact that larger amounts of filamentous actin require a longer time for depolymerization. Moreover, it has been reported that the disassembly of filamentous actin is slower in the presence of Arp2/3 [34], and actin reannealing is more prominent in the case of dense Arp2/3-rich networks [35,36].

A time-delayed feedback model captures the relations between response amplitude and polymerization time scales.—We present a dynamical model that recovers our main experimental findings, in particular, (i) the peak value of polymerized actin in a cell varies with the amount of Arp2/3, (ii) the polymerization time is independent of the actin amplitude, and (iii) the depolymerization time grows with increasing actin amplitude. Our model is purely phenomenological. It was designed to qualitatively reproduce the dynamical features of our experimental observations. We do not intend to capture any of the molecular details of the underlying biological mechanism with this model.

Consistent with previous experimental observations [18], we found that the dynamics of depolymerization promoters, such as Aip1, follow that of LimE with a delay τ [21]. This suggests that the filamentous actin concentration $L(t)$ can be modeled by an equation of the form

$$\frac{dL(t)}{dt} = k_+(t)L(t) - k_-B(t)L(t), \tag{1}$$

where the depolymerization rate $B(t)$ is a function of $L(t-\tau)$. In the regime of weak oscillations, $B(t)$ was taken to be proportional to $L(t-\tau)$, and the resulting model provided a simplified description of actin dynamics close to the onset of oscillations [18]. In its original form, however, the model does not properly reproduce the increase of the depolymerization time with the actin amplitude, clearly shown in Fig. 3(b). To account for this effect, we assume that the rate of actin depolymerization saturates when $L(t-\tau)$ is large:

$$B(t) = \begin{cases} L(t-\tau) & : L(t-\tau) < C_{\max}, \\ C_{\max} & : L(t-\tau) \geq C_{\max}. \end{cases} \tag{2}$$

Below $C_{\max}$, the amount of depolymerization proteins is approximately proportional to $L(t-\tau)$. Under strong stimulation, $L(t)$ increases, but the amount of depolymerization proteins saturates at $C_{\max}$. Note that the form of B in Eq. (2) could be replaced, without any qualitative change, by a sigmoidal dependence.

The function $k_+(t)$ describes the polymerization rate, which is constant in the absence of any stimulation and increases for a short while after a pulse of cAMP is delivered: $k_+(t) = k_+^0 + k_s(t)$, where k_+^0 is the polymerization rate in the absence of stimulation and $k_s(t)$ denotes a transient increase in the polymerization rate due to the stimulus. The increase in the polymerization rate with the amount of activated Arp2/3 in the cell, clearly seen in Fig. 3(c), can be simply taken into account by varying the magnitude of $k_s(t)$ to reproduce the observed variability in the actin amplitude.

Consistent with the experimental observations, simulations of Eqs. (1) and (2) show that, upon varying the increase in the polymerization rate k_s after stimulation, the polymerization time remains constant (T_p is slightly longer than the delay τ [21]), whereas the depolymerization time increases with the amplitude (black lines in Fig. 4). The success of our model at capturing qualitatively our main experimental observations backs the essential assumption that Arp2/3, via $k_+(t)$, is a key ingredient to explain the cell-to-cell variability in the response to a stimulation.

According to the current view, the response of chemotactic cells can be modeled by an upstream excitable signaling network that is linked to a downstream actin machinery with oscillatory dynamics [24,37,38]. Previously observed actin oscillations with a period of 10–20 s [18,24] are a consequence of this downstream oscillatory system and can be described by a delay differential equation [18] or by the normal form of a supercritical Hopf bifurcation when operating close to onset [26]. Also, the observations of the present Letter reflect properties of the actin cytoskeleton, so that we chose an adapted form of the delay differential equation model to account for our new findings. Only the threshold behavior is not captured by our actin model. As threshold responses are a typical hallmark of an excitable system, we ascribe this property to the dynamics of the upstream signaling network.

Even though Eq. (2) captures well the key experimental observations, several open questions remain. In particular, according to the time-delay model, the polymerization time is determined by the time shift τ between the actin peak and the peak in the cortical localization of depolymerization promotors such as Aip1 and coronin. However, our data did not show a correlation between T_p and τ [21]. This could be due to the complex nature of the reactions controlling polymerization and depolymerization in the actin system.

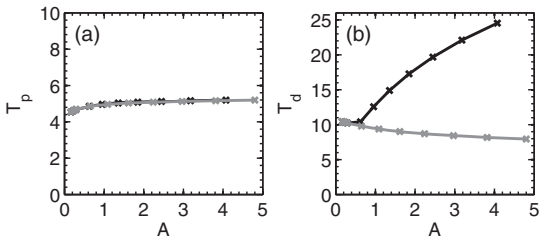

FIG. 4. Simulations of model Eqs. (1) and (2) with a finite value of $C_{\max} = 1.4$ (black line) and in the absence of saturation $C_{\max} \gg 1$ (gray line). They capture the constant T_p as well as the increasing T_d for increasing A in the case of Eq. (2). Parameters are $k_+^0 = 0.2$, $\tau = 4$, $k_- = 0.2$, and $C_{\max} = 1.4$. Simulation traces are shown in Ref. [21].

As this is an obvious limitation of our simplified approach, it invites further future investigation. Also, explaining the constant polymerization time from molecular considerations remains a key issue to substantiate our phenomenological approach. We also stress that only a more detailed investigation, at the molecular level, could confirm the underlying assumption that actin dynamics is triggered once the transduction system has been excited, because actin polymerization and the signal transduction system may be coupled together by feedback loops [39].

In summary, our findings highlight pronounced cell-to-cell variability in the receptor-induced actin response of chemotactic cells. The response threshold as well as the amplitude and time scales of the response above the threshold vary strongly from cell to cell. However, with respect to the polymerization and depolymerization times, the amplitude follows well-defined relations. In particular, a wide range of different amplitudes caused by variations in Arp2/3 activity is robustly mapped onto a narrow interval of polymerization times. While the origin of fluctuations in the Arp2/3 activity remains unknown, the constant polymerization time can be seen as a prerequisite for the reliable formation of membrane protrusions irrespective of large variations in the receptor input signal or the upstream signaling pathway.

This work was funded by the Deutsche Forschungsgemeinschaft (DFG) SFB 937 "Collective behavior of soft and biological matter," subproject A9.

*eberhard.bodenschatz@ds.mpg.de
†beta@uni-potsdam.de

[1] A. J. Ridley, M. A. Schwartz, K. Burridge, R. A. Firtel, M. H. Ginsberg, G. Borisy, J. T. Parsons, and A. R. Horwitz, Science **302**, 1704 (2003).
[2] P. J. M. Van Haastert and P. N. Devreotes, Nat. Rev. Mol. Cell Biol. **5**, 626 (2004).
[3] C. Beta and K. Kruse, Annu. Rev. Condens. Matter Phys. **8**, 239 (2017).
[4] P. J. M. Van Haastert, J. Cell Sci. **123**, 3031 (2010).
[5] M. Gerhardt, M. Ecke, M. Walz, A. Stengl, C. Beta, and G. Gerisch, J. Cell Sci. **127**, 4507 (2014).
[6] S. J. Annesley and P. R. Fisher, Mol. Cell. Biochem. **329**, 73 (2009).
[7] E. C. Woodhouse, R. F. Chuaqui, and L. A. Liotta, Cancer **80**, 1529 (1997).
[8] C. C. Bleul and T. Boehm, European Journal of Immunology **30**, 3371 (2000).
[9] E. Theveneau, L. Marchant, S. Kuriyama, M. Gull, B. Moepps, M. Parsons, and R. Mayor, Dev. Cell **19**, 39 (2010).
[10] M. O. Li, Y. Y. Wan, S. Sanjabi, A.-K. L. Robertson, and R. A. Flavell, Annu. Rev. Immunol. **24**, 99 (2006).
[11] P. N. Devreotes and S. H. Zigmond, Annual Review of Cell Biology **4**, 649 (1988).
[12] L. Song, S. M. Nadkarni, H. U. Boedeker, C. Beta, A. Bae, C. Franck, W.-J. Rappel, W. F. Loomis, and E. Bodenschatz, Eur. J. Cell Biol. **85**, 981 (2006).
[13] C. J. Wang, A. Bergmann, B. Lin, K. Kim, and A. Levchenko, Sci. Signal. **5**, ra17 (2012).
[14] A. Samadani, J. Mettetal, and A. van Oudenaarden, Proc. Natl. Acad. Sci. U.S.A. **103**, 11549 (2006).
[15] L. Pelkmans, Science **336**, 425 (2012).
[16] I. Sadler, A. W. Crawford, J. W. Michelsen, and M. C. Beckerle, J. Cell Biol. **119**, 1573 (1992).
[17] T. Bretschneider, S. Diez, K. Anderson, J. Heuser, M. Clarke, A. Müller-Taubenberger, J. Köhler, and G. Gerisch, Curr. Biol. **14**, 1 (2004).
[18] C. Westendorf, J. Negrete, A. J. Bae, R. Sandmann, E. Bodenschatz, and C. Beta, Proc. Natl. Acad. Sci. U.S.A. **110**, 3853 (2013).
[19] A. Bae, C. Beta, and E. Bodenschatz, Lab Chip **9**, 3059 (2009).
[20] C. Beta, D. Wyatt, W.-J. Rappel, and E. Bodenschatz, Anal. Chem. **79**, 3940 (2007).
[21] See Supplemental Material at http://link.aps.org/supplemental/10.1103/PhysRevLett.119.148101 for more details, which includes Refs. [18,20,22,23].
[22] D. Qin, Y. N. Xia, and G. M. Whitesides, Nat. Protoc. **5**, 491 (2010).
[23] B. J. Nolen, N. Tomasevic, A. Russell, D. W. Pierce, Z. Jia, C. D. McCormick, J. Hartman, R. Sakowicz, and T. D. Pollard, Nature (London) **460**, 1031 (2009).
[24] C.-H. Huang, M. Tang, C. Shi, P. A. Iglesias, and P. N. Devreotes, Nat. Cell Biol. **15**, 1307 (2013).
[25] O. Hoeller, J. E. Toettcher, H. Cai, Y. Sun, C.-H. Huang, M. Freyre, M. Zhao, P. N. Devreotes, and O. D. Weiner, PLoS Biol. **14**, e1002381 (2016).
[26] J. Negrete, A. Pumir, H.-F. Hsu, C. Westendorf, M. Tarantola, C. Beta, and E. Bodenschatz, Phys. Rev. Lett. **117**, 148102 (2016).
[27] T. D. Pollard and G. G. Borisy, Cell **113**, 549 (2003).
[28] T. D. Pollard, L. Blanchoin, and R. D. Mullins, Annu. Rev. Biophys. Biomol. Struct. **29**, 545 (2000).
[29] C. Hug, P. Y. Jay, I. Reddy, J. G. Mcnally, P. C. Bridgman, E. L. Elson, and J. A. Cooper, Cell **81**, 591 (1995).
[30] E. O. Potma, W. P. de Boeij, L. Bosgraaf, J. Roelofs, P. J. M. van Haastert, and D. A. Wiersma, Biophys. J. **81**, 2010 (2001).
[31] X. H. Xu, M. Meier-Schellersheim, X. M. Jiao, L. E. Nelson, and T. Jin, Mol. Biol. Cell **16**, 676 (2005).
[32] C. Janetopoulos, T. Jin, and P. Devreotes, Science **291**, 2408 (2001).
[33] C. A. Elzie, J. Colby, M. A. Sammons, and C. Janetopoulos, J. Cell Sci. **122**, 2597 (2009).
[34] L. Blanchoin, T. D. Pollard, and R. D. Mullins, Curr. Biol. **10**, 1273 (2000).
[35] T. Miyoshi and N. Watanabe, Cytoskeleton **70**, 179 (2013).
[36] T. Miyoshi, T. Tsuji, C. Higashida, M. Hertzog, A. Fujita, S. Narumiya, G. Scita, and N. Watanabe, J. Cell Biol. **175**, 947 (2006).
[37] M. Nishikawa, M. Horning, M. Ueda, and T. Shibata, Biophys. J. **106**, 723 (2014).
[38] Y. Miao, S. Bhattacharya, M. Edwards, H. Cai, T. Inoue, P. A. Iglesias, and P. N. Devreotes, Nat. Cell Biol. **19**, 329 (2017).
[39] A. T. Sasaki, C. Chun, K. Takeda, and R. A. Firtel, J. Cell Biol. **167**, 505 (2004).